Dynamic Simulations of Three-Phase Squirrel-Cage Induction Motors under One Phase Loss of Supply Voltage Using LTspice Program

Pichai Aree[1]

[1]Department of Electrical and Computer Engineering, Faculty of Engineering, Thammasat School of Engineering, Thammasat University, Pathumthani, 12120, Thailand

apichai@engr.tu.ac.th

Abstract

Analyzing the dynamic responses of induction motors in the event of one-phase loss in the power supply is essential. Traditional direct-quadrature(*dq*)-axis dynamic models of induction motor, commonly employed in commercial-graded software tools lack support for such analyses. This paper introduces a hybrid ABC/dq model, maintaining the stator-circuit representation in ABC frame of reference. The presented model is fully implemented in the freeware LTspice circuit simulator software and validated against the commercially available Matlab/Simulink software. The comparative result reveals a strong agreement in a satisfactory manner. The hybrid model provides significant flexibility for investigating various scenarios without the need for explicit mathematical formulations. For example, the study results indicate that introducing a neutral return wire between the motor and power supply can mitigate single-phasing and enhance the motor performance in the event of phase loss. Moreover, incorporating a capacitor in series with the phase-loss winding can substantially reduce unbalanced issues to an acceptable level.

Keywords: Dynamic simulations, induction motors, unbalanced conditions, single-phasing, LTspice program.

1. Introduction

The industrial world greatly values the induction motors due to its affordability in terms of both initial expenses and upkeep. They span a range from less than one horsepower to several thousand horsepower. While most induction motors are intended for use with a balanced three-phase power source, deviations in system voltages from the standard can be quite significant. This variance has a detrimental effect on the stable operation of the motor (Faiz, et al., 2004; El-Kharashi et al., 2019). Fluctuations in voltage lead to imbalances in the currents flowing through the motor's stator windings, resulting in overheating. The elevated temperatures subsequently contribute to a decrease in the motor's overall lifespan.

An imbalance in phases can stem from factors like an unstable power supply from the utility, an uneven distribution in a transformer bank, blown fuses, thermal overloads, damaged wiring, worn-out contacts, or mechanical malfunctions (Kersting, 2001; Sutherland & Short, 2006). Additionally, the interruption of a fault by automatic circuit reclosers can lead to single-phasing operation (Sudha & Anbalagan, 2007). As the smart grid concept gains traction for enhancing reliability, a growing trend involves selectively interrupting and reclosing only the lines affected by faults, ensuring that the unaffected phases remain functional (Agamloh et al., 2014). In such scenarios, induction motor loads are subjected to the phenomenon of single phasing (Kocman et al., 2023).

It is widely recognized that three-phase induction motors can still operate in the event of a loss of one of the three-phase supply voltages (Giceva et al., 2018). During this period, these motors exhibit behavior akin to that of a single-phase motor because their star points remain unconnected to the power supply's neutral point, resulting in a floating configuration. Consequently, the motor's torque experiences a rapid decline, potentially

leading to overheating and subsequent damage (Ferreira et al., 2018). In many cases, it becomes crucial to sustain motor operation using the remaining two-phase voltages, especially when critical industrial processes cannot be abruptly halted to prevent damage. This research underscores the significance of the neutral lead, which can be swiftly switched to establish a connection between the supply source and motor's star points when one phase of the supply voltages is lost (Enache et al., 2019).

In order to investigate the dynamic performance of induction motors during unbalanced condition, the conventional dq-axis model is commonly used. The model describes the voltage, current, and flux in the stator and rotor circuits using direct (*d*) and quadrature (*q*) axes reference frame (Krause et al., 2002). However, applying this reference frame to the stator winding becomes complicated when assessing motor behavior under the single-phasing condition (Zenginobuz, 2001). For example, attempting to adapt the stator wiring configurations according to the *d*- and *q*-axis model perspective is not practical in such situations. Consequently, it is not surprising that widely-used commercial-grade software packages like Matlab and PSCAD (MathWorks, 2023; PSCAD, 2022) do not readily support this specific analysis.

To address this challenge, this research paper adopts a hybrid ABC/dq model. This model specifically transforms the current, voltage, and flux variables of the rotor circuit into the *d*- and *q*-axis, while still maintaining the stator circuit-oriented model within the ABC frame of reference. Although originally proposed by Pillay and Levin in 1995, this paper provides a detailed derivation of the model and corrects typographical errors in mathematical expressions. Furthermore, the paper offers a comprehensive, step-by-step guide on implementing the ABC/dq model in the LTspice freeware simulator. The simulation results obtained from the employed LTspice model are then compared

and validated against those obtained from commercially available Matlab/Simulink software. The exceptional flexibility of the developed LTspice model is demonstrated under various study scenarios, particularly when one phase of the supply voltage is missing. Additionally, this paper examines the impact of the neutral return wire on motor dynamic performance and investigates the use of an additional capacitor to mitigate motor's unbalance issues when experiencing a phase loss.

2. Mathematical Model of Three-Phase Induction Motor

To analysis the dynamic behaviors of induction motors, the circuit models in ABC/abc frame of reference is used as shown in Figure 1. It consists of three-phase stator and rotor windings placing along the magnetic axes, namely A, B, C and a, b, c, respectively. The stator phase voltages (v_{sA}, v_{sB}, v_{sC}) drives currents (i_{sA}, i_{sB}, i_{sC}) in each phase to produce the total magnetic fluxes (ψ_{sA}, ψ_{sB}, ψ_{sC}). These fluxes are employed to generate induced voltages in the rotor body, which drives the rotor currents (i_{ra}, i_{rb}, i_{rc}) to build additional fluxes (ψ_{ra}, ψ_{rb}, ψ_{rc}). The voltage equations of stator and rotor windings can be expressed as (Krause et al., 2002),

$$\mathbf{v}_{sABC} = \mathbf{r_s}\,\mathbf{i}_{sABC} + \frac{d\boldsymbol{\psi}_{sABC}}{dt} \tag{1}$$

$$\mathbf{v}_{rabc} = \mathbf{r_r}\,\mathbf{i}_{rabc} + \frac{d\boldsymbol{\psi}_{rabc}}{dt} \tag{2}$$

Where $\mathbf{r_s}$ and $\mathbf{r_r}$ are diagonal matrices, containing the stator (R_s) and rotor (R_r) resistances, respectively.

$$\mathbf{r_s} = \begin{bmatrix} R_s & 0 & 0 \\ 0 & R_s & 0 \\ 0 & 0 & R_s \end{bmatrix}, \qquad \mathbf{r_r} = \begin{bmatrix} R_r & 0 & 0 \\ 0 & R_r & 0 \\ 0 & 0 & R_r \end{bmatrix}$$

The column vectors of voltages, currents, and fluxes in (1) and (2), can be defined as,

$$\mathbf{v}_{sABC} = \begin{bmatrix} v_{sA} \\ v_{sB} \\ v_{sC} \end{bmatrix} = \begin{bmatrix} V_{\max}\cos(\omega_s t) \\ V_{\max}\cos(\omega_s t - 2\pi/3) \\ V_{\max}\cos(\omega_s t + 2\pi/3) \end{bmatrix}, \qquad \mathbf{v}_{rabc} = \begin{bmatrix} v_{ra} \\ v_{rb} \\ v_{rc} \end{bmatrix},$$

$$\mathbf{i}_{sABC} = \begin{bmatrix} i_{sA} \\ i_{sB} \\ i_{sC} \end{bmatrix}, \quad \mathbf{i}_{rabc} = \begin{bmatrix} i_{ra} \\ i_{rb} \\ i_{rc} \end{bmatrix}, \qquad \boldsymbol{\psi}_{sABC} = \begin{bmatrix} \psi_{sA} \\ \psi_{sB} \\ \psi_{sC} \end{bmatrix}, \quad \boldsymbol{\psi}_{rabc} = \begin{bmatrix} \psi_{ra} \\ \psi_{rb} \\ \psi_{rc} \end{bmatrix}$$

$V_{\max}$ is the peak voltage. ω_s is electrical speed in rad/sec. The fluxes in (1) and (2) can be written as,

$$\boldsymbol{\psi}_{sABC} = \mathbf{L_{ss}}\,\mathbf{i}_{sABC} + \mathbf{L_{sr}}\,\mathbf{i}_{rabc} \tag{3}$$

$$\boldsymbol{\psi}_{rabc} = \mathbf{L_{rs}}\,\mathbf{i}_{sABC} + \mathbf{L_{rr}}\,\mathbf{i}_{rabc} \tag{4}$$

Where,

$$\mathbf{L_{ss}} = \begin{bmatrix} L_{ls}+L_{sr} & -0.5L_{sr} & -0.5L_{sr} \\ -0.5L_{sr} & L_{ls}+L_{sr} & -0.5L_{sr} \\ -0.5L_{sr} & -0.5L_{sr} & L_{ls}+L_{sr} \end{bmatrix}, \qquad \mathbf{L_{rr}} = \begin{bmatrix} L_{lr}+L_{sr} & -0.5L_{sr} & -0.5L_{sr} \\ -0.5L_{sr} & L_{lr}+L_{sr} & -0.5L_{sr} \\ -0.5L_{sr} & -0.5L_{sr} & L_{lr}+L_{sr} \end{bmatrix},$$

$$\mathbf{L_{sr}} = L_{sr}\begin{bmatrix} \cos(\theta_r) & \cos(\theta_r+120^o) & \cos(\theta_r-120^o) \\ \cos(\theta_r-120^o) & \cos(\theta_r) & \cos(\theta_r+120^o) \\ \cos(\theta_r+120^o) & \cos(\theta_r-120^o) & \cos(\theta_r) \end{bmatrix}$$

Where L_{ls} and L_{lr} are flux leakages of stator and rotor, respectively. L_{sr} is mutual flux between stator and rotor when electrical angular displacement (θ_r) in Figure 1 is set to zero. It is noted that $\mathbf{L_{rs}}$ in (4) is equal to $(\mathbf{L_{sr}})^{\mathbf{T}}$.

To derive the hybrid ABC/dq model, it is necessary convert the electrical quantities of rotor circuit from the ABC-axis to dq-axis using the following transformation matrix (Krause et al., 2002).

$$f_{dqr} = K_r\, f_{abcr} \tag{5}$$

where,

$$K_r = \sqrt{\frac{2}{3}}\begin{bmatrix} \cos(\theta_r) & \cos(\theta_r+120^o) & \cos(\theta_r-120^o) \\ \sin(\theta_r) & \sin(\theta_r+120^o) & \sin(\theta_r-120^o) \end{bmatrix}$$

Applying the transformation matrix in (5) to convert the rotor quantities in (2), (3), and (4) gives,

$$\mathbf{v}_{rdq} = \mathbf{r_r}\,\mathbf{i}_{rdq} + K_r \frac{d}{dt}\{K_r^{-1}\boldsymbol{\psi}_{rdq}\} \tag{6}$$

$$\boldsymbol{\psi}_{sABC} = \mathbf{L_{ss}}\,\mathbf{i}_{sABC} + \mathbf{L_{sr}} K_r^{-1}\,\mathbf{i}_{rdq} \tag{7}$$

$$\boldsymbol{\psi}_{rdq} = K_r \mathbf{L_{sr}}\,\mathbf{i}_{sABC} + K_r \mathbf{L_{rr}} K_r^{-1}\,\mathbf{i}_{rdq} \tag{8}$$

After substituting (7) into (1), and then re-arranging, the expression of stator voltages in the ABC-axis frame of reference can be written in compact form as,

$$\begin{bmatrix} v_{sA} \\ v_{sB} \\ v_{sC} \end{bmatrix} = \underbrace{R_s \begin{bmatrix} 1 & 0 & 0 \\ 0 & 1 & 0 \\ 0 & 0 & 1 \end{bmatrix} \begin{bmatrix} i_{sA} \\ i_{sB} \\ i_{sC} \end{bmatrix}}_{\textit{voltage drop}} + \underbrace{L_s \begin{bmatrix} 1 & 0 & 0 \\ 0 & 1 & 0 \\ 0 & 0 & 1 \end{bmatrix} \frac{d}{dt} \begin{bmatrix} i_{sA} \\ i_{sB} \\ i_{sC} \end{bmatrix}}_{\textit{transformer voltage}} + \underbrace{M \begin{Bmatrix} 1 & 0 \\ -0.5 & \sqrt{3}/2 \\ -0.5 & -\sqrt{3}/2 \end{Bmatrix} \frac{d}{dt} \begin{bmatrix} i_{rd} \\ i_{rq} \end{bmatrix}}_{\textit{induced voltage due to rotor current}} \tag{9}$$

After substituting (8) into (6), and then re-arranging, the expression of rotor voltages in the dq-axis frame of reference can be written in compact form as,

$$\begin{bmatrix} v_{rd} \\ v_{rq} \end{bmatrix} = \underbrace{R_r \begin{bmatrix} 1 & 0 \\ 0 & 1 \end{bmatrix} \begin{bmatrix} i_{rd} \\ i_{rq} \end{bmatrix}}_{\textit{voltage drop}} + \underbrace{L_r \begin{bmatrix} 1 & 0 \\ 0 & 1 \end{bmatrix} \frac{d}{dt} \begin{bmatrix} i_{rd} \\ i_{rq} \end{bmatrix}}_{\textit{transformer voltage}} + \underbrace{M \begin{Bmatrix} 1 & -0.5 & -0.5 \\ 0 & \sqrt{3}/2 & -\sqrt{3}/2 \end{Bmatrix} \frac{d}{dt} \begin{bmatrix} i_{sA} \\ i_{sB} \\ i_{sC} \end{bmatrix}}_{\textit{induced voltage due to stator current}} + \underbrace{\omega_r L_r \begin{bmatrix} 0 & 1 \\ -1 & 0 \end{bmatrix} \begin{bmatrix} i_{rd} \\ i_{rq} \end{bmatrix} + M\omega_r \begin{bmatrix} 0 & \sqrt{3}/2 & -\sqrt{3}/2 \\ -1 & 0.5 & 0.5 \end{bmatrix} \begin{bmatrix} i_{sA} \\ i_{sB} \\ i_{sC} \end{bmatrix}}_{\textit{speed voltage}} \tag{10}$$

Where $L_s = L_{ls} + L_m$, $L_r = L_{lr} + L_m$, $M = \sqrt{(2/3)}L_m$, $L_m = 1.5L_{sr}$. It is noted that L_s and L_r are self-inductances of stator and rotor, respectively, while L_m is related to mutual inductance. It can be seen from (9) that the hybrid model of induction motor consists of stator currents in the ABC-axis and rotor currents in the dq-axis. Lastly, the slow dynamic variable of induction motor is related to the angular velocity. The rate of change of motor' mechanical speed (ω_m) in rad/sec can be expressed as,

$$J\frac{d\boldsymbol{\omega}_m}{dt} = T_e - B\boldsymbol{\omega}_m - T_m \tag{11}$$

Where J and B are moment of inertia and friction coefficients, respectively. The electrical torque T_e can be expressed in term of ABC frame of reference as (Pillay &

Levin, 1995),

$$T_e = -\frac{P}{2} L_{sr} \begin{pmatrix} (i_{sA} i_{ra} + i_{sB} i_{rb} + i_{sC} i_{rc}) \sin(\theta_r) + (i_{sA} i_{rb} + i_{sB} i_{rc} + i_{sC} i_{ra}) \sin(\theta_r + 2\pi/3) + \\ (i_{sA} i_{rc} + i_{sB} i_{ra} + i_{sC} i_{rb}) \sin(\theta_r - 2\pi/3) \end{pmatrix} \tag{12}$$

After transforming the rotor current in (12) into dq-axis components, the motor induced torque can be re-written as,

$$T_e = \frac{P}{2} M \left(i_{rq} (0.5 i_{sB} + 0.5 i_{sC} - i_{sA}) + \frac{\sqrt{3}}{2} i_{rd} (i_{sB} - i_{sC}) \right) \tag{13}$$

According to the IEEE standard (IEEE Task Force, 1995), the driven-load torque of motor can be written by,

$$T_m = T_{m0} \left(A(\omega_m / \omega_{sm})^2 + B(\omega_m / \omega_{sm}) + C \right) \tag{14}$$

T_{m0} is regarded as the mechanical torque at synchronous speed (ω_{sm}). The coefficients A, B, and C indicate the portion of torque changing with the speed squared, speed, and constant, respectively.

3. LTspice Model Implementation of Induction Motor

This section presents an effective approach for utilizing the LTspice circuit simulator software to model the three-phase induction motors. Essentially, mathematical expressions presented in (9) and (10) describe the stator and rotor terminal voltages in the ABC and dq axes, respectively. By eliminating the time-varying inductance and maintaining a constant inductance matrix over time, this hybrid ABC/dq model offers significant reductions in computational time. The comprehensive top-level schematic model of induction motor is displayed in Figure 2a, with the corresponding subcircuit depicted in Figure 2b.

To implement the motor model within the LTspice environment, the effects of voltage drops due to stator winding resistance and transformer voltage caused by self-flux linkages, can be represented by combining resistive elements (R_s) in series with inductive elements (L_s), as illustrated in the subcircuit model in Figure 2b. The

availability of three-phase coils with six terminals (A and An, B and Bn, C and Cn) allows easy emulation of the physical wiring with both star and delta connections, as shown in Figure 2a. With this implemented model, the state variables employed as i_{sA}, i_{sB}, and i_{sC} in corresponding to the physical current flowing in each coil, can be directly examined.

Similarly, the rotor circuit can be represented by series elements consisting of resistances (R_r) and inductances (L_r). Since the rotor voltage equation in (10) contains speed voltage terms, the current-dependent voltage sources (V), specifically Bd and Bq, are employed to represent them within the d- and q-axis rotor circuits, as described in Figure 2b. Furthermore, the mathematical expressions (9) and (10) reveal that the model is significantly simplified since the mutual inductances among the ABC-axes stator and dq-axes rotor circuits are invariant and independent of the rotor angular position. In this context, the main effects of these mutual inductances, as enclosed in curly brackets in equations (9) and (10), can be easily incorporated into the LTspice program using the SPICE directive command and mutual inductance statement, as illustrated in Figure 2b.

To complete the LTspice model, the motor's electromechanical dynamics must be integrated into the subcircuit. To accomplish this, the electrical analogies of mechanical systems (Akbaba, 2021) are fully utilized. Therefore, the rate of change of dynamic motion in (11) can be represented through an electrical circuit model, as shown in Figure 2b, labeled as the "Electromechanical dynamics". The electrical and mechanical torques in (13) and (14) are modeled using current-dependent current sources, specifically Bte and Btm, respectively. The expressions of these current sources are fully provided in Figure 2b.

4. Results and Discussions

To ensure a correctness of the presented mathematical model, this section provides a comparative analysis of simulation results between the hybrid ABC/dq model and the conventional dq/dq model under balanced and unbalanced conditions.

4.1 Model Validation under Balanced Condition

To validate the ABC/dq mathematical model under the LTspice environment, a three-phase squirrel-cage induction motor rated at 2.2kW, 4.7A and 400V are used. The motor's parameters are defined using the SPICE directive commands, as depicted in Figure 2b. The stator circuits of three-phase motor are connected in wye configuration, with the star point directly linked to that of the power source, as illustrated in Figure 2a. To enable a comparison, the widely-used Simscape model, found Matlab/Simulink commercial software, is employed to represent the motor under test using the conventional dq-axis frame of reference as depicted in Figure 3a. It's worth noting that the motor operates without a mechanical shaft load and is subjected to a balanced applied voltage.

To evaluate and compare the motor's dynamic responses, the profiles of torque, speed, and current (phase A), simulated from both LTspice and Simscape models, are plotted as shown in Figure 4a. It is important to highlight that the simulation outcome derived from the LTspice computational engine is exported as a standard text file to Matlab. This facilitates the simultaneous generation of multiple plots within the same figure. Notably, the motor exhibits torque pulsations during the accelerating interval. The motor reaches steady-state condition at 270 milliseconds, corresponding to a decline in the starting current. Importantly, a strong correspondence between the LTspice and commercial Simscape models is consistently observed across the entire range of torque, speed, and current responses, from transient to steady-state conditions.

4.2 Model Validation under Unbalanced Condition

Further validations are conducted while the motor is operating under an unbalanced condition resulting from a phase-loss fault. In this case, the stator current of the open-phase winding should ideally be zero. Assessing the motor's dynamic performance under this condition presents certain limitations with various commercial software tools. For example, the Simscape model of motor in Figure 3a lacks the option to disconnect or remove one phase of the power supply in the event of a phase loss. Additionally, it has limitations in examining the unbalanced neutral current flowing through a wire connected between the star points of the stator windings and the three-phase power sources.

In order to compare the simulation responses between the implemented LTspice circuit and the Matlab/Simulink models, the primary equations in (9) and (10) are further reformulated in state-space form, as shown in A3-A4 in Appendix A. The motor model is subsequently constructed in Matlab/Simulink environment using these two equations, along with those in (11), (13), and (14), and is presented in block-diagram representation in Figure 3b.

In this study, the assumption is made that that the C-phase voltage of motor is lost (i_C=0) while it is running at full load amperage (FLA). To simulate such a condition, switches are employed to alter the coefficients matrices from their normal values, K11 and K21 in (A-3) and (A-4), to their faulty counterparts, K11f and K21f, where the stator’s resistance related to the disconnected C-phase is specifically set to a very high value to prevent the flow of current.

From the circuit simulation perspective, the proposed LTspice model can be straightforwardly modified to simulate the phase loss event without conducting a tedious

formulating the expressions in (9) and (10) into the state-space form. The switch model named MYSW is employed to cut off the C-phase current directly from the power source at t=0.6sec, as illustrated in Figure 3c (left side). The neutral point between motor and power supply is connected through a very small resistance, denoted as RN. Importantly, it should be noted that the motor's shaft torque (referred to as Btm) is characterized by a constant torque profile (T_{m0}=12.4Nm, A=0, B=0, C=1).

After performing the dynamic simulation, the plots of torque, speed, and currents are displayed in Figures 4b-4e, respectively. It is evident that there is strong agreement in torque, speed, and current profiles between the LTspice and Matlab/Simulink models during occurrence of the phase loss, thus confirming the accuracy of the proposed LTspice model.

4.3 Motor Performance Under One-Phase Loss

This section explores the dynamic performance of induction motors when experiencing phase-loss scenarios. Using the circuit LTspice simulator, the motor's performance with and without grounding the star point can be straightforwardly examined by simply connecting or disconnecting this point to a 0V reference point. Typically, it is advisable not to ground the motor's neutral point to prevent unbalanced current flow into the earth (Basu, Yusuf, 1999). Nevertheless, in this section, the potential advantage of introducing the neutral wire to transport the unbalanced currents back to the supply against the single-phasing issues can be investigated.

Initially, it is assumed that the wye-connected 2.2kW motor is operating at its FLA value. This motor drives mechanical load characterized by the constant-torque type. As illustrated in Figure 4b-4e, it is intriguing to note that the motor can generate an output torque of 12.4Nm to drive the given mechanical loads after a successful acceleration

through a direct-on-line starting at 0.5 seconds. The simulated stator current waveforms in Figure 4d-4e confirm that the motor draws an FLA of 4.7A rms or 6.65A peak.

However, at 0.6 seconds, when the C-phase supply voltage is disconnected, the motor experiences torque oscillation at twice supply frequency (100Hz), as depicted in Figure 4b. These oscillation results in uncomfortable torsional pulsation, vibration, and noise. Under this context, it is worthwhile to investigate the impact of employing a neutral return wire. The comparative responses of torque and speed in steady-state condition can be fully observed in Figure 5a and 5b. It becomes evident that the degree of oscillation in electromagnetic torque decreases when the motor continues to run with inclusion of the neutral wire. In this scenario, Figure 5b demonstrates that the motor can operate in a higher-speed region, affirming an increased power output and improved speed regulation. Therefore, the utilization of a neutral conductor during the one-phase loss undoubtedly enhances the motor's ability to handle the mechanical load.

Next, it is of interest to investigate the line current under this particular scenario. The comparative responses of currents for the A and B-phases can be displayed in Figure 5c and 5d. It becomes evident that the line currents of the remaining two phases experience a significant increase. Notably, Figure 5d demonstrates that the motor current worsens, reaching 1.97 times of FLA value when the motor's star point is left floating. The currents in A and B-phases are completely out of phase with each other, signifying that they return to the power supply through the lines. This result confirms that the motor runs in a single-phasing mode with line-to-line voltage across two stator windings, leading to a substantial decrease in its output power.

However, when a return path is established, the unbalanced neutral current of 0.4A rms (2.7 peak) flows back to the power supply as depicted in Figure 5c. This return current

contributes to diminishing the excess line currents, with the A- and B-phase, still showing values of 1.67 and 1.8 times of the FLA, respectively (Figure 5c). It is noted that the motor requires more input currents to maintain the same level of mechanical output torque, which can result in increased winding temperatures. Over time, this can cause insulation damage and reduce the motor's lifespan.

It is of interes to explore the motor’s performance under the phase loss when driving different types of mechanical loads. In this case, the expression in (14), fully implemented via the LTspice subcircuit (Figure 2b), allows for investigation of various types of mechanical shaft loads. Two types of them, namely constant-torque and speed-squared-torque types, are examined. The assumption is made such that the motor is initially operated at the same speed under two distinct mechanical loads, with the torque profile being proportional to the square of the speed (T_{m0}=12.4Nm, A=1, B=0, C=0) and a constant torque (T_{m0}=11.5086Nm, A=0, B=0, C=1), prior to experiencing the phase-loss condition. The total inertia of motor plus load is set equally.

Once the simulations are completed, the motor’s electrical torque, driven-load torque, and speed are plotted as shown in Figure 6. It is evident that a different rate of acceleration is experienced by the motor. The constant-torque load exhibits the longest starting time. Importantly, Figure 6 indicates that the greatest fall in speed is primarily associated with the motor characterized by the constant-torque load profile. Hence, a greater amount of input current is always drawn by the motor equipped with this type of load during the phase-loss interval.

4.4 Motor Performance Under Phase Loss with Capacitor

Based on the presented results, the single-phasing is not a favorable condition due to excessive input currents. To address this issue, it is necessary to take the motor out of

service by activating the main circuit breaker. In certain applications, continuous operation may be required to power a critical load for a specific duration. Consequently, this section explores the impact of introducing an additional capacitor to mitigate the degree of current imbalance. Utilizing the LTspice circuit model depicted in Figure 3c (right), it becomes straightforward to incorporate an extra capacitor between the A-phase and C-phase terminals. The analysis described in (Tanthanuch, Aree, 2020) is then utilized to determine the optimal size of the supplementary capacitor. In this particular instance, a 40uF capacitor has been selected. The simulated profiles of current, torque, and speed, are plotted as depicted in Figure 7.

Figure 7a clearly demonstrates that by introducing an additional capacitor, there is a significant reduction in the current magnitudes in the remaining two phases. The running amperages readings for the A- and B-phases are approximately 3.81A rms (5.4A peak) and 5.37Arms (7.6A peak), respectively. The current in the neutral return conductor is now only 0.42A rms (0.6A peak), indicating a substantial decrease in the degree of unbalance in line currents. The highest level of overcurrent is reduced to just 1.14 times of the motor's FLA, allowing the motor to operate for a specific duration without exceeding its thermal capacity. In this context, if the motor has a service factor of 1.15, continuous operation becomes possible.

Furthermore, it is interesting to assess the motor's performance in terms of induced torque and operating speed. Figure 7b reveals a notable decrease in the torsional pulsations caused by the unbalanced currents. In this scenario, the useful FFT tool in LTspice software tool enables comprehensive exploration of the harmonic contents within the torque signal. Figure 7c displays the results of FFT analysis, revealing two prominent peaks at 50Hz and 100Hz. The distinctive maximum (10dB) at the second

harmonic (100Hz) is attributed to a loss of one phase in the supply voltage. This notable peak is greatly attenuated as a result of improved balance in the remaining line currents achieved through the supplementary capacitor. The substantial improvement in torque and current restores the motor's performances to its original state, within the same operating speed range, as clearly seen in Figure 7d.

5. Conclusion

This paper focuses on the mathematical modelling of induction motor using the hybrid ABC/dq frame of reference. The implementation of the ABC/dq model is comprehensively demonstrated within LTspice, a powerful, fast, and free circuit simulator software. This model has undergone validation against Simscape and Matlab/Simulink models, resulting in excellent agreement observed in a satisfactory manner. This approach facilitates the exploration of highly unbalanced conditions that arise from the phase loss under various stator winding configurations, with and without the neutral return wire and additional capacitor.

The findings emphasize the importance of having a neutral return wire to counteract single-phasing problem when a phase is lost. Moreover, adding a capacitor in series with the phase-loss winding of the motor can substantially reduce unbalanced issue of the running currents to an acceptable level, thereby improving the motor's operational torque performance, speed regulation, and efficiency.

In summary the implementation of the hybrid ABC/dq model into LTspice circuit simulator allows for excellent waveform analysis, enabling engineers to gain valuable insights into the motor behaviors and dynamic performances across various configurations. This approach reduces both the time and cost associated with developing

explicit mathematical formulations of each unique configuration. It addresses limitations found in the commercial software tools that rely on the traditional dq/dq model.

6. Apendix A

This appendix presents the state-space form of hybrid ABC/dq model. The expressions in (9) and (10) can be written in compact form as,

$$\bar{\mathbf{i}}_{sABC} = \mathbf{A}_{11}\,\mathbf{i}_{sABC} + \mathbf{A}_{12}\,\bar{\mathbf{i}}_{rdq} + \mathbf{B}_{11}\mathbf{v}_{sABC} \tag{A-1}$$

$$\bar{\mathbf{i}}_{rdq} = \mathbf{A}_{21}\,\bar{\mathbf{i}}_{sABC} + \mathbf{A}_{22}\,\bar{\mathbf{i}}_{rdq} + \boldsymbol{\omega}_r\mathbf{F}_{21}\,\mathbf{i}_{sABC} + \boldsymbol{\omega}_r\mathbf{F}_{22}\,\mathbf{i}_{rdq} \tag{A-2}$$

Where,

$$\mathbf{A}_{11} = -\frac{R_s}{L_s}\begin{bmatrix}1&0&0\\0&1&0\\0&0&1\end{bmatrix}\quad \mathbf{A}_{12} = -\frac{M}{L_s}\begin{bmatrix}1&0\\-0.5&\sqrt{3}/2\\-0.5&-\sqrt{3}/2\end{bmatrix}\quad \mathbf{B}_{11} = \frac{1}{L_s}\begin{bmatrix}1&0&0\\0&1&0\\0&0&1\end{bmatrix}$$

$$\mathbf{A}_{22} = -\frac{R_r}{L_r}\begin{bmatrix}1&0&0\\0&1&0\\0&0&1\end{bmatrix}\quad \mathbf{A}_{21} = -\frac{M}{L_s}\begin{bmatrix}1&-0.5&-0.5\\0&\sqrt{3}/2&-\sqrt{3}/2\end{bmatrix}\quad \mathbf{F}_{22} = \begin{bmatrix}0&-1\\1&0\end{bmatrix}\quad \mathbf{F}_{21} = -\frac{M}{L_r}\begin{bmatrix}0&\sqrt{3}/2&-\sqrt{3}/2\\-1&0.5&0.5\end{bmatrix}$$

The overline symbol on top of the variables denotes differential operator *d/dt*. By substituting (A-2) into (A-1), the derivative of stator current can be re-arranged as,

$$\bar{\mathbf{i}}_{sABC} = \left(\mathbf{K}_{11} + \boldsymbol{\omega}_r\mathbf{K}_{11w}\right)\mathbf{i}_{sABC} + \left(\mathbf{K}_{12} + \boldsymbol{\omega}_r\mathbf{K}_{12w}\right)\mathbf{i}_{rdq} + \mathbf{U}_{11}\mathbf{v}_{sABC} \tag{A-3}$$

Where

$$\mathbf{K}_{11} = \left(\mathbf{I}_{3\times3} - \mathbf{A}_{12}\mathbf{A}_{21}\right)^{-1}\mathbf{A}_{11} \qquad \mathbf{K}_{11w} = \left(\mathbf{I}_{3\times3} - \mathbf{A}_{12}\mathbf{A}_{21}\right)^{-1}\mathbf{A}_{12}\mathbf{F}_{21}$$

$$\mathbf{K}_{12} = \left(\mathbf{I}_{3\times3} - \mathbf{A}_{12}\mathbf{A}_{21}\right)^{-1}\mathbf{A}_{12}\mathbf{A}_{22} \qquad \mathbf{K}_{12w} = \left(\mathbf{I}_{3\times3} - \mathbf{A}_{12}\mathbf{A}_{21}\right)^{-1}\mathbf{A}_{12}\mathbf{F}_{22} \qquad \mathbf{U}_{11} = \left(\mathbf{I}_{3\times3} - \mathbf{A}_{12}\mathbf{A}_{21}\right)^{-1}\mathbf{B}_{11}$$

By substituting (A-1) into (A-2), the derivative of rotor current can be re-arranged as,

$$\bar{\mathbf{i}}_{rdq} = \left(\mathbf{K}_{21} + \boldsymbol{\omega}_r\mathbf{K}_{21w}\right)\mathbf{i}_{sABC} + \left(\mathbf{K}_{22} + \boldsymbol{\omega}_r\mathbf{K}_{22w}\right)\mathbf{i}_{rdq} + \mathbf{U}_{22}\mathbf{v}_{sABC} \tag{A-4}$$

Where,

$$\mathbf{K}_{22} = \left(\mathbf{I}_{2\times2} - \mathbf{A}_{21}\mathbf{A}_{12}\right)^{-1}\mathbf{A}_{22} \qquad \mathbf{K}_{22w} = \left(\mathbf{I}_{2\times2} - \mathbf{A}_{21}\mathbf{A}_{12}\right)^{-1}\mathbf{F}_{22}$$

$$\mathbf{K}_{21} = \left(\mathbf{I}_{2\times2} - \mathbf{A}_{21}\mathbf{A}_{12}\right)^{-1}\mathbf{A}_{21}\mathbf{A}_{11} \qquad \mathbf{K}_{21w} = \left(\mathbf{I}_{2\times2} - \mathbf{A}_{21}\mathbf{A}_{12}\right)^{-1}\mathbf{F}_{21} \qquad \mathbf{U}_{22} = \left(\mathbf{I}_{2\times2} - \mathbf{A}_{21}\mathbf{A}_{12}\right)^{-1}\mathbf{A}_{21}\mathbf{B}_{11}$$

7. Acknowledgment

The author gratefully acknowledges the financial support provided by Faculty of Engineering, Thammasat School of Engineering, Thammasat University, contract No. 004/2566.

8. References

Agamloh, E. B., Peele, S., Grappe, J. (2014). Induction Motor Single-Phasing Performance Under Distribution Feeder Recloser Operations. *IEEE Trans. Industry Applications*, *50*(2), 1568-1576.

Akbaba, M. (2021). Modeling and simulation of dynamic mechanical systems using electric circuit analogy. *Turkish Journal of Engineering*, *5*(3), 111-117.

Basu, K. P., Yusuf, S. (1999). A novel method of starting a 3-phase induction motor with one phase out from the source of supply. *International Journal of Electrical Engineering Education*, *6*(1), 25-30.

El-Kharashi, E., Massoud, J. G., Al-Ahmar, M. A. (2019). The impact of the unbalance in both the voltage and the frequency on the performance of single and cascade induction motors. *Energy*, 181, 561-575.

Enache, S., Campenanu, A., Vlad, I., Enache, M. A. (2019). Aspects regarding tests of three-phase asynchronous motors with single-phase supply. *16th Conference on Electrical Machines, Drives and Power Systems (ELMA)*, Varna, Bulgaria, 1-6

Giceva, I. Z., Sarac, V. J., Gelev, S. A., Cingoski, V. T. (2018). Single phasing of three phase induction motors under various load conditions. *23rd International Scientific-Professional Conference on Information Technology (IT)*, Zabljak, Montenegro, 1-4.

Faiz, J., Ebrahimpour, H., Pillay, P. (2004). Influence of unbalanced voltage on the steady-state performance of a three-phase squirrel-cage induction motor. *IEEE Trans. Energy Conversion*, *19*(4), 657–662.

Ferreira, F. J. T. E., Silva, A. M., de Almeida, A. T. (2018). Single-phasing protection of line-operated motors of different efficiency casses. *IEEE Trans. Industry Applications*, *54*(3), 2071-2084.

IEEE Task Force. (1995). Load representation for dynamic performance. *IEEE Trans. Power Systems*, *10*(3), 1302-1313.

Kersting, W. H. (2001). Causes and effects of unbalanced voltages serving an induction motor. *IEEE Trans. Industry Applications*, *37*(1), 165-170.

Kocman, S., Demel, L., Orság P., Hrbáč, R. (2023) Single phasing simulation of asynchronous motor. *23rd International Scientific Conference on Electric Power Engineering (EPE)*, Brno, Czech Republic, 1-5.

Krause, P., Wasynczuk, O., Sudhoff, S., Pekarek, S. (2013). *Analysis of Electric Machinery and Drive Systems*. New Jersey, IEEEPress, John Wiley&Sons.

The MathWorks Inc. (2022). MATLAB version: 9.13.0 (R2022b), Natick, Massachusetts: The MathWorks Inc. Retrieved from https://www.mathworks.com/help/sps/ug/three-phase-asynchronous-machine.html

Pillay, P. Levin, V. (1995). Mathematical models for induction machines. *IEEE Industry Applications Conference Thirtieth IAS Annual Meeting*, Orlando, FL, USA, 606-616.

Manitoba HVDC Research Centre, “PSCAD/EMTDC: Electromagnetic transients program including dc systems,”, 1994.

PSCAD User’s Guide. (2022) Manitoba Res. Ctr., Winnipeg, MB, Canada. Retrieved from https://www.pscad.com/knowledge-base/article/49

Sudha, M., Anbalagan, P. (2007). A novel protecting method for induction motor against faults due to voltage unbalance and single phasing. *33rd Annual conference of the IEEE Industrial Electronics Society*, Taipei, Taiwan, 1144-1148.

Sutherland, P. E., Short, T. A. (2006). Effect of single-phase reclosing on industrial loads. *IEEE Industry Applications Conference Forty-First IAS Annual Meeting*, Tempa, FL, USA, 2636-2644.

Tanthanuch, N., Aree, P., (2020). Techniques for improving torque performance of three phase induction motor under single phasing condition using capacitor and neutral wire. *The Journal of KMUTNB*, *30*(1), 49-59.

Zenginobuz, G., Cadirci, I., Ermis, M., Barlak, C. (2001). Soft starting of large induction motors at constant current with minimized starting torque pulsations. *IEEE Trans. Industry Applications*, *37*(5), 1334-1347.

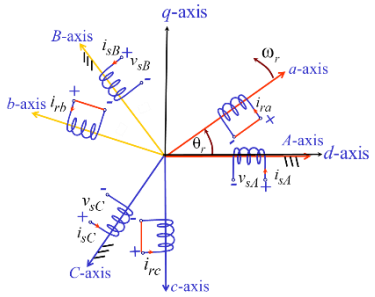

Figure 1 Construction of induction motor.

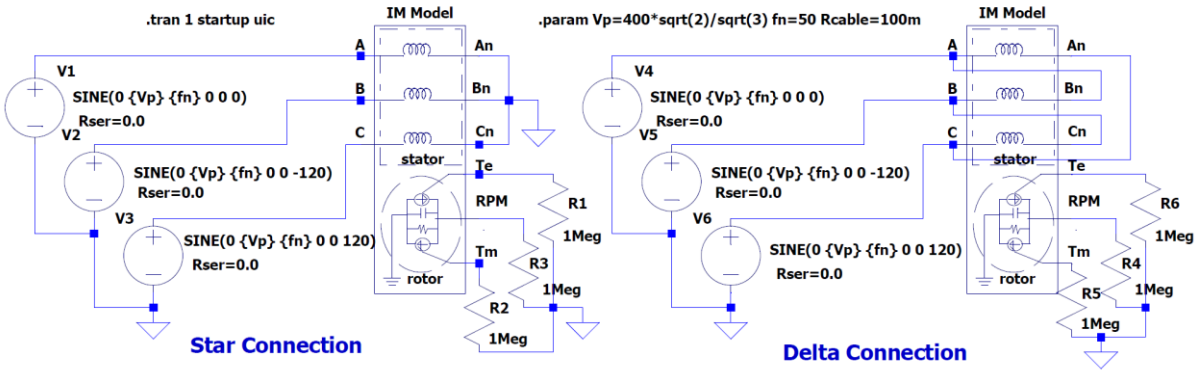

(a) Top-level schematic of induction motor model

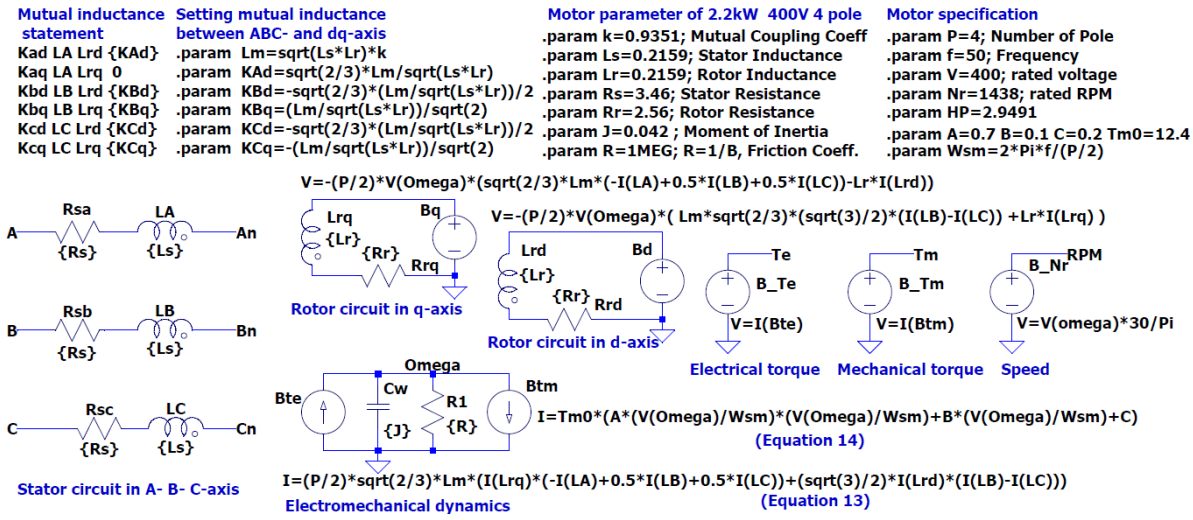

(b) Schematic of subcircuit of induction motor model

Figure 2 Representation of induction motor in LTspice software.

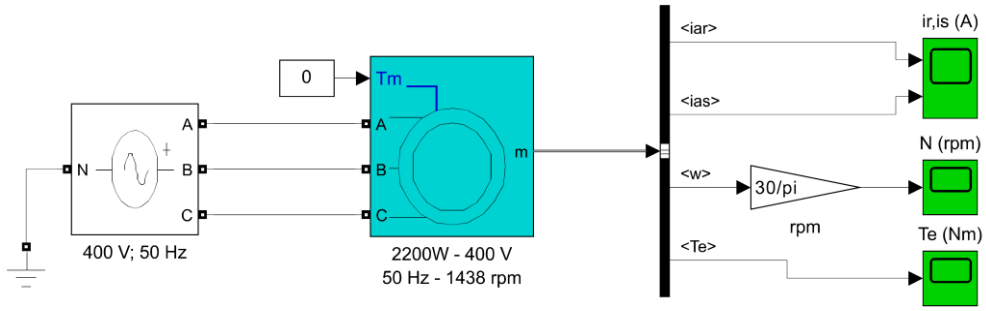

(a) Simcape model of induction motor

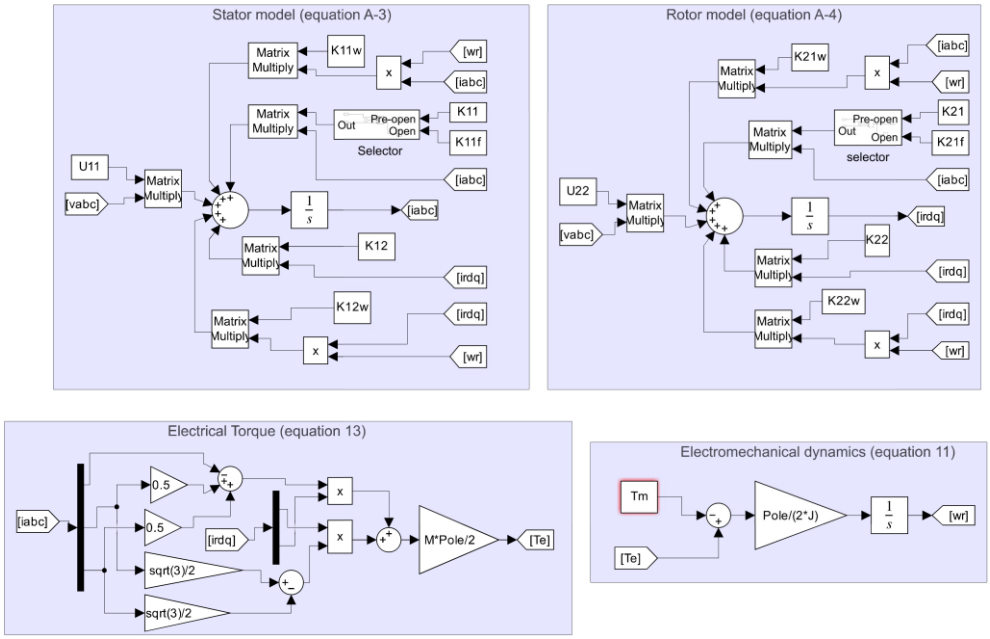

(b) Matlab/Simulink model of induction motor

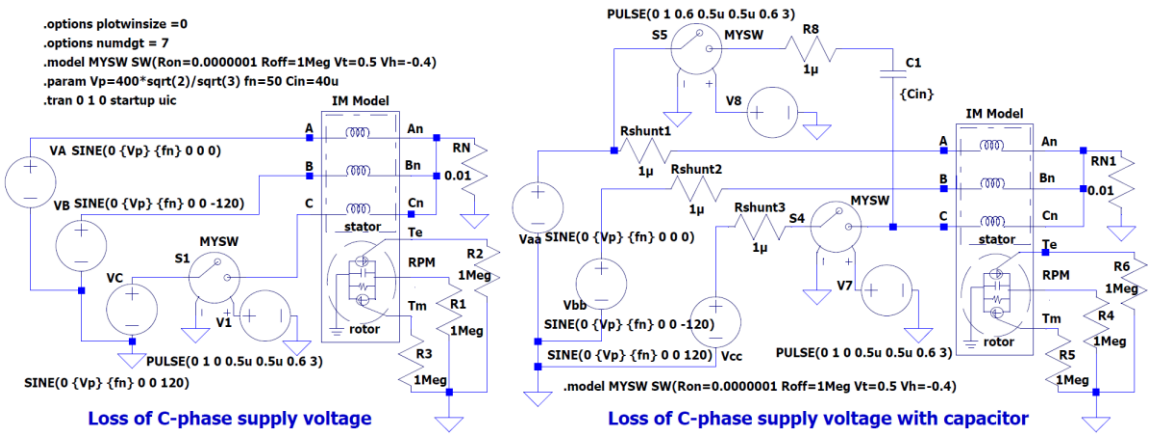

(c) LTspice model of induction motor

Figure 3 Simcape and Simulink models of induction motor.

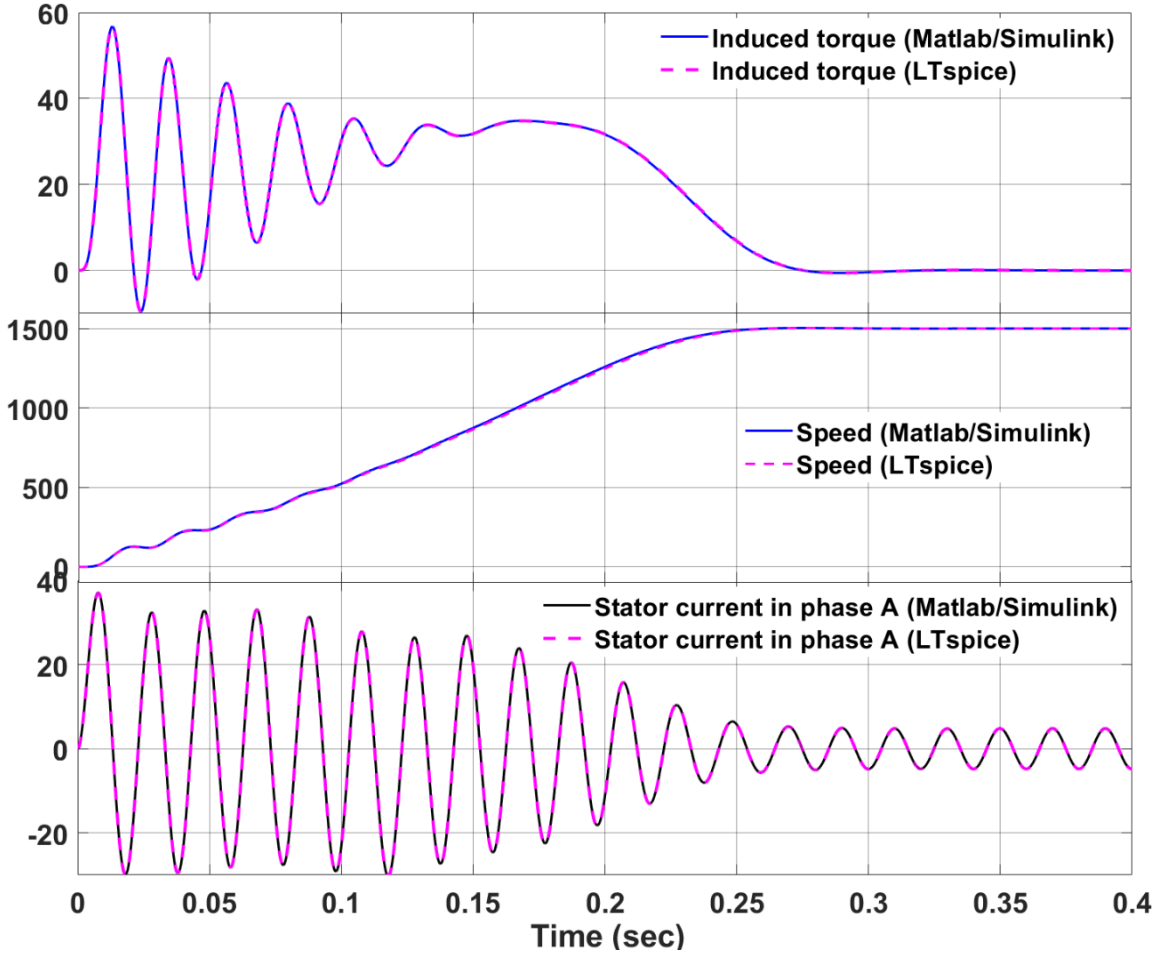

(a) Torque, speed, and current profiles under balanced condition

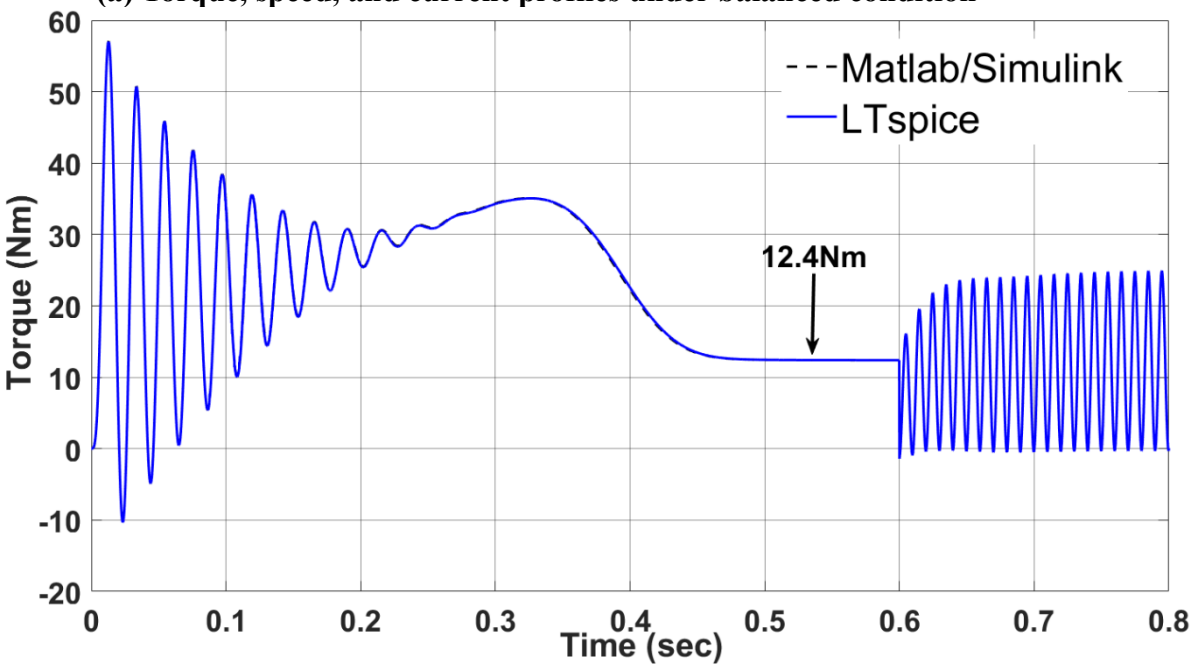

(b) Torque profile under loss of C-phase voltage

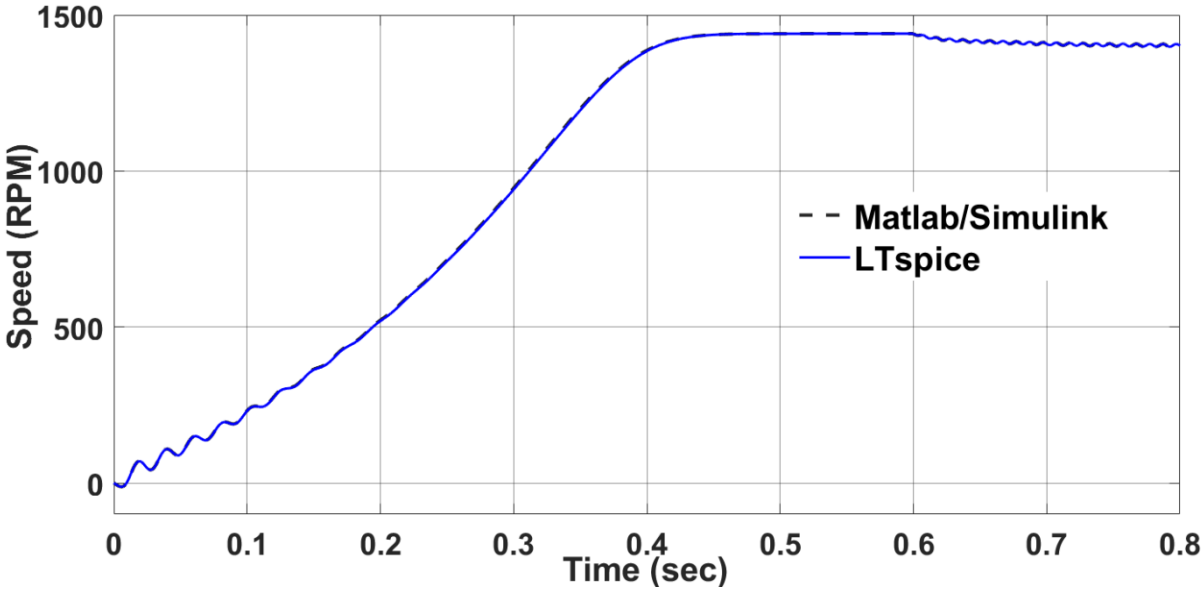

(c) Speed profile under loss of C-phase voltage

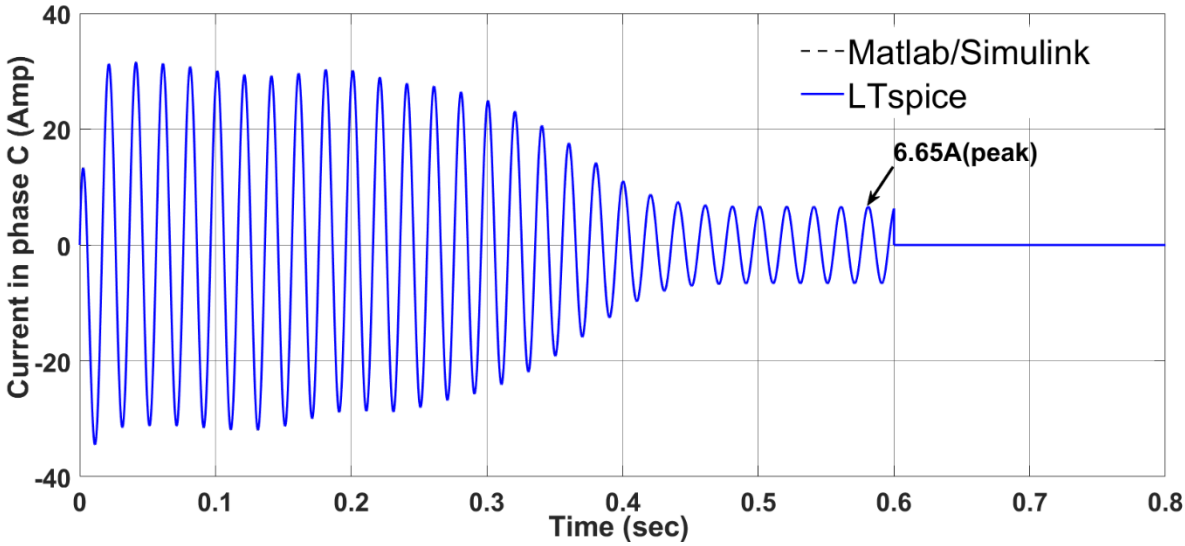

(d) Current in C-phase under loss of C-phase voltage

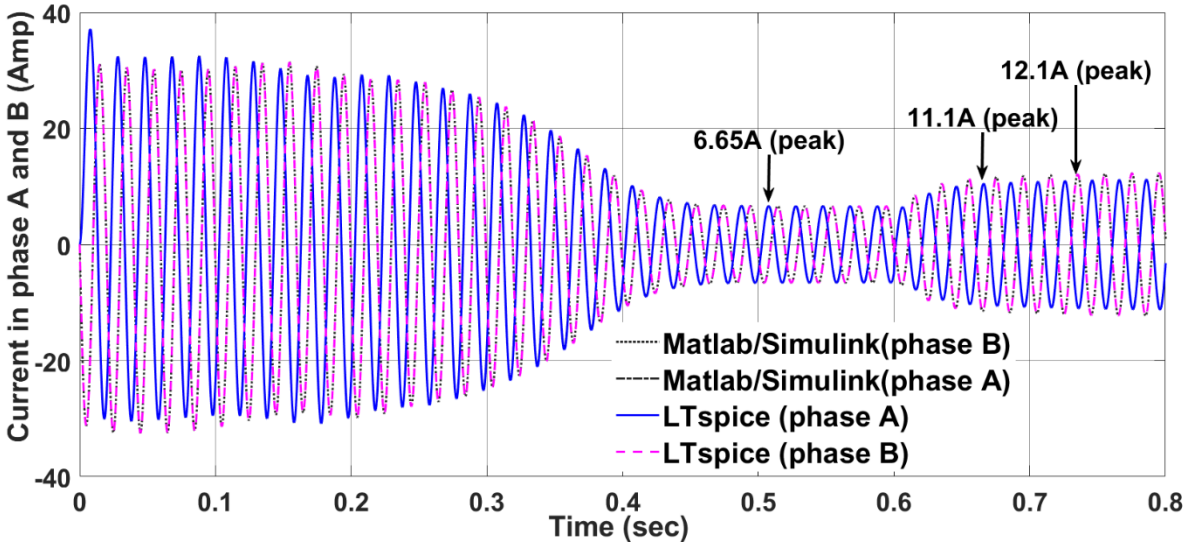

(e) Currents in A- and B-phases under loss of C-phase voltage

Figure 4 Torque and current profiles under balanced and unbalanced conditions.

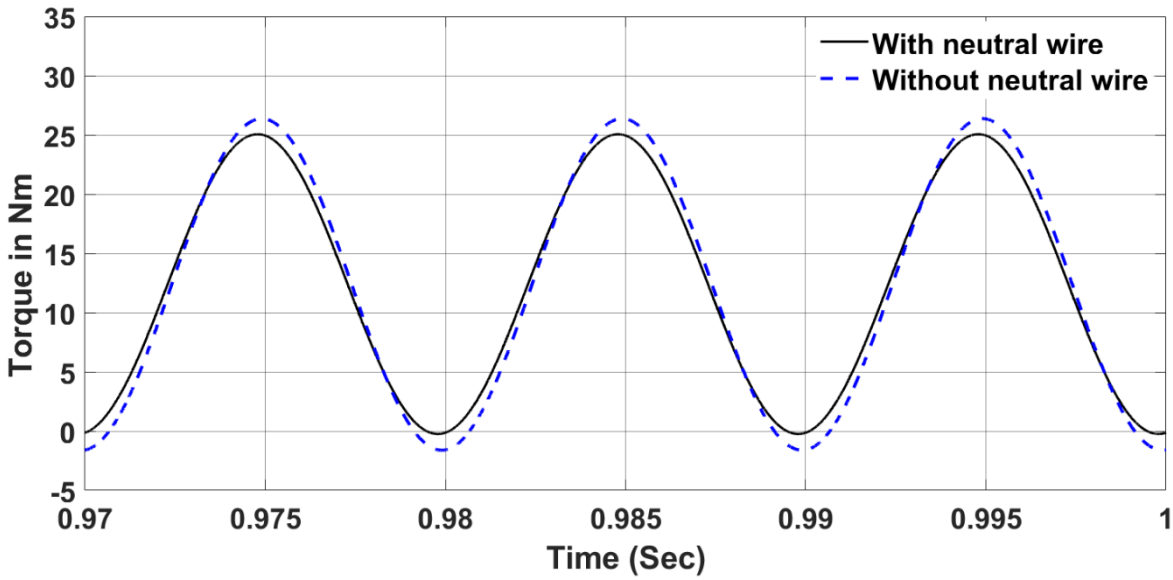

(a) Torque profile with and without neutral wire

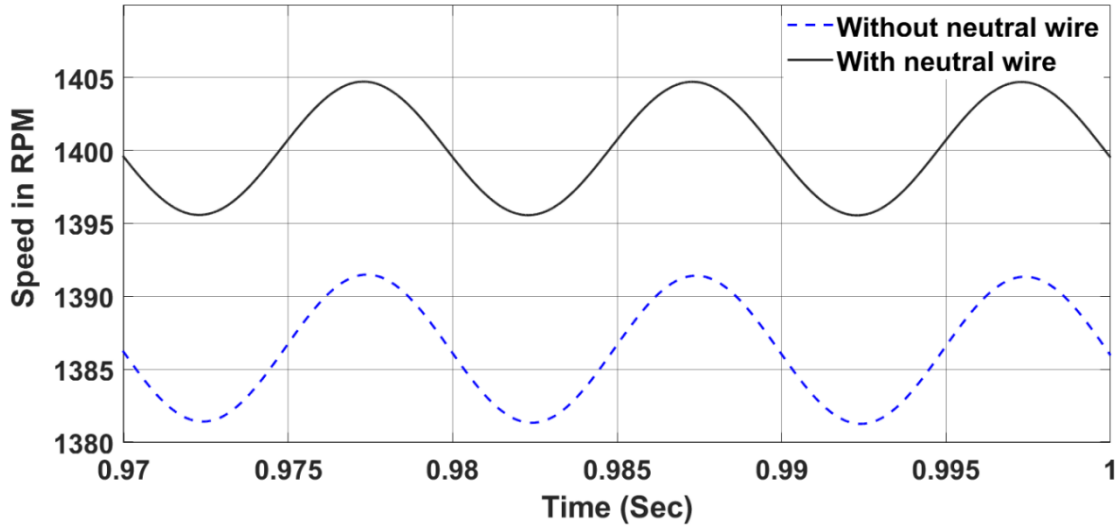

(b) Speed profile with and without neutral wire

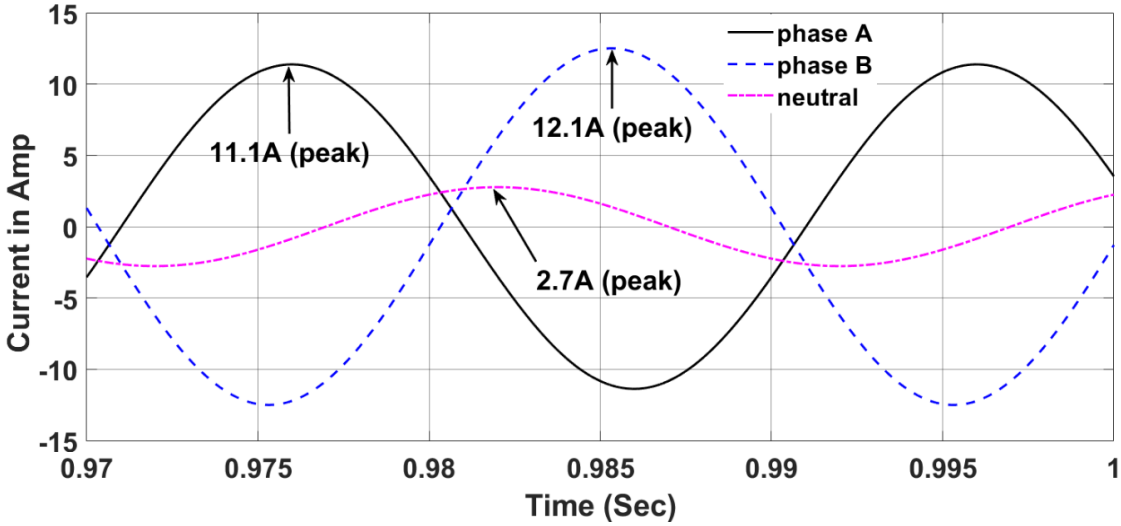

(c) Current profile with neutral wire

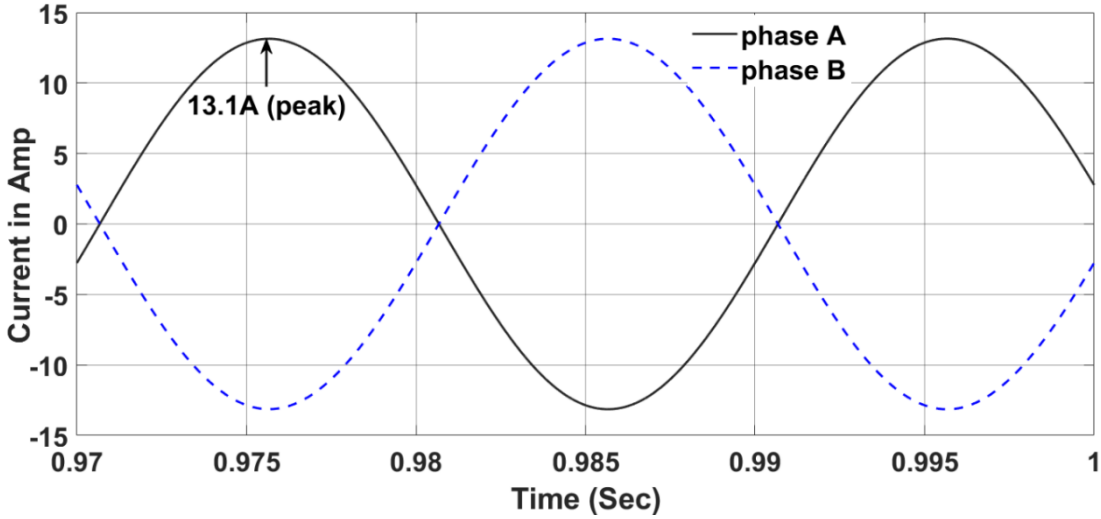

(d) Current profile without neutral wire

Figure 5 Torque, speed, current profiles with and without neutral wire.

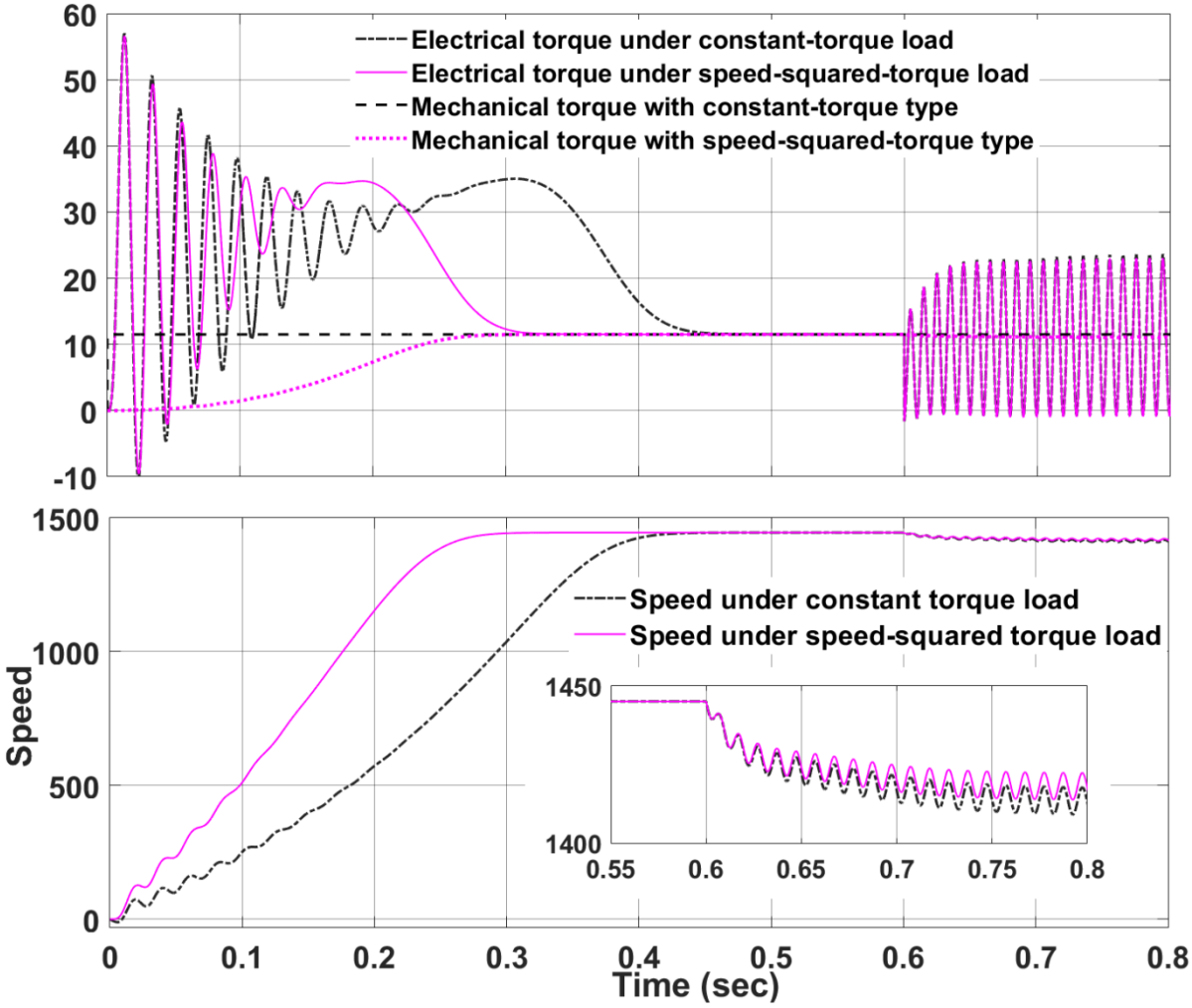

Figure 6 Torque, speed profiles with different profiles of mechanical loads.

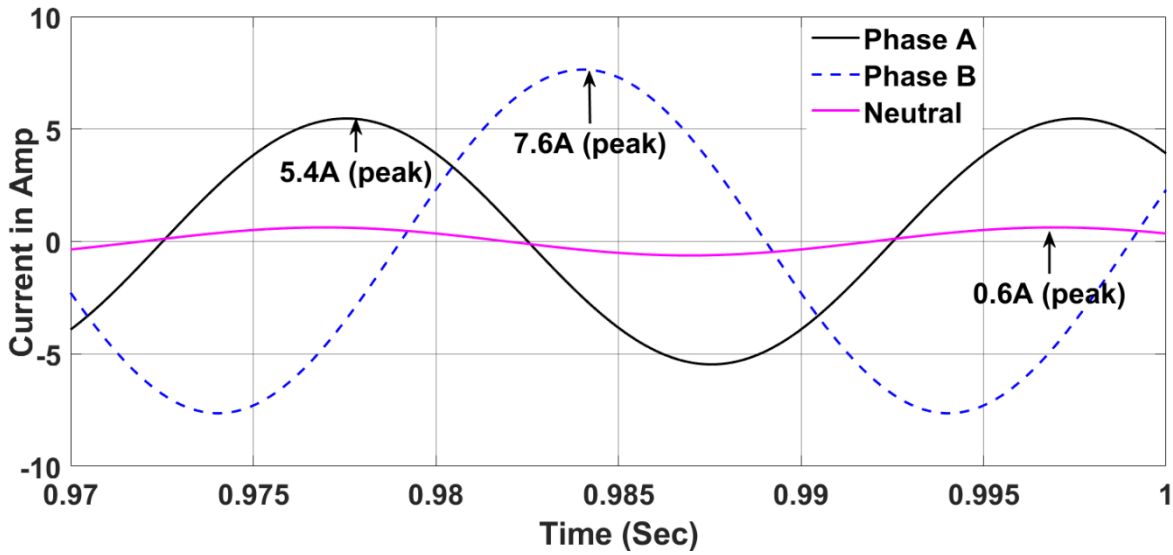

(a) Current profile

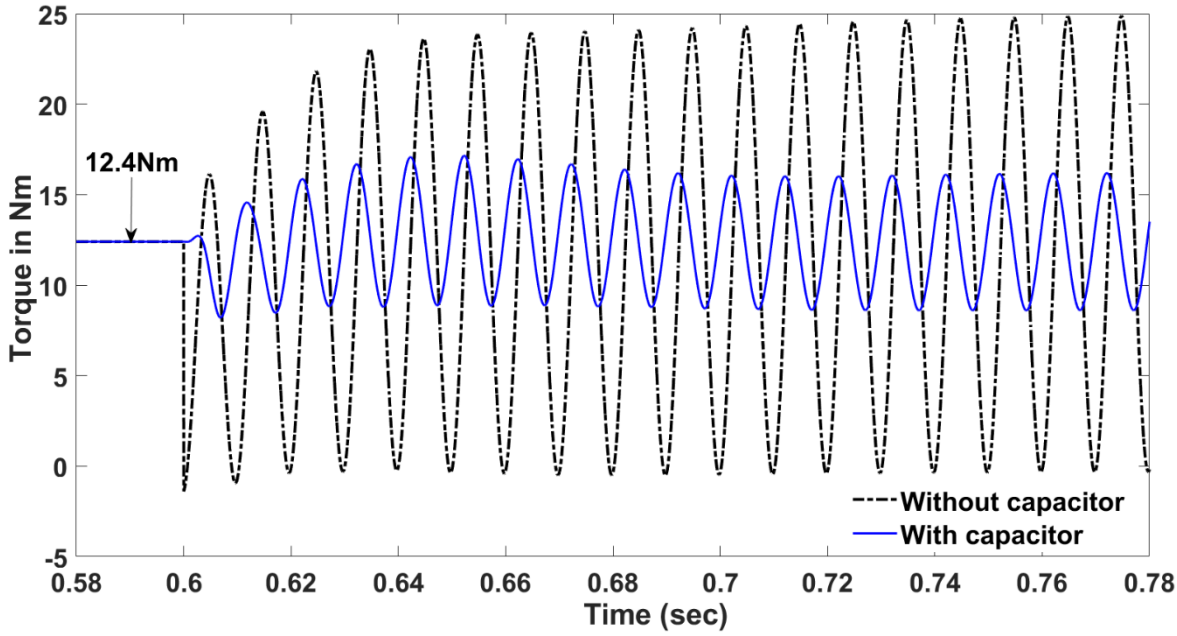

(b) Torque profile

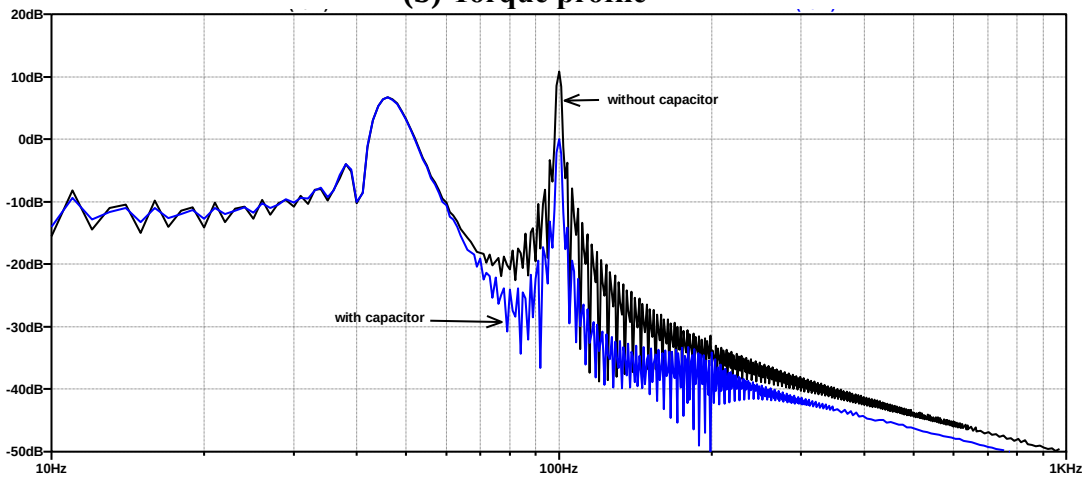

(c) FFT of torque profiles

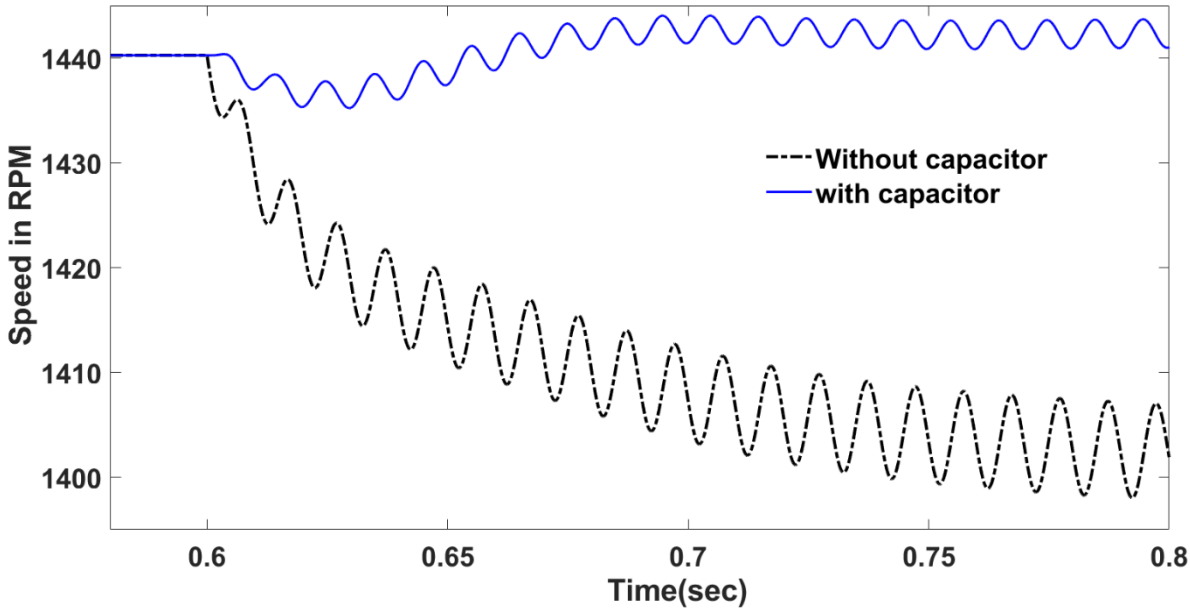

(d) Speed profile

Figure 7 Current, torque, speed profiles with and without capacitor installation.